Role of ^{18}F-DCFPyL PET/CT in patients with suspected prostate cancer

Tingting Zhang[1] MD,
Shuye Yang[1] MD, PhD,
Lili Lin[1] MD,
Shuo Wang[2] MD,
Dan Xia[2] MD, PhD,
Donghe Chen[1] MD,
Guolin Wang[1] MD,
Kui Zhao[1] MD,
Xinhui Su[1] MD, PhD

1. PET Center, Department of Nuclear Medicine, The First Affiliated Hospital, School of Medicine, Zhejiang University, Hangzhou 310003, China
2. Department of Urology Surgery, The First Affiliated Hospital, School of Medicine, Zhejiang University, Hangzhou 310003, China

Keywords: Suspected prostate cancer - ^{18}F-DCFPyL - PET/CT - Diagnosis - Staging

Corresponding authors:
Kui Zhao MD,
PET Center, Department of Nuclear Medicine
The First Affiliated Hospital, School of Medicine, Zhejiang University
79 Qingchun Road, Hangzhou 310003, China.
Phone: 86-0571-87236428
Fax: 86-0571-87236428.
zhaokui0905@zju.edu.cn

Xinhui Su MD, PhD,
PET Center, Department of Nuclear Medicine
The First Affiliated Hospital, School of Medicine, Zhejiang University
79 Qingchun Road, Hangzhou 310003, China.
Phone: 86-0571-87236428
Fax: 86-0571-87236428.
suxinhui@zju.edu.cn

Received:
27 October 2021
Accepted revised:
14 February 2022

Abstract

Objective: Fluorine-18-2-(3-{1-carboxy-5-[(6-18F-flfluoro-pyridine-3-carbonyl)-amino]-pentyl}-ureido)-pentanedioic acid (^{18}F-DCFPyL), a novel positron emission tomography/computed tomography (PET/CT) radiotracer that binds to the prostate specific membrane antigen (PSMA), is increasingly used for biochemically recurrent prostate cancer diagnostics. However, the ^{18}F-DCFPyL characteristics of suspected prostate cancer (SPCa) have been even more rarely described. Herein, in this retrospective study, we describe the clinical impact of ^{18}F-DCFPyL PET/CT imaging in SPCa. **Subjects and Methods:** We retrospectively evaluated the data of 56 SPCa patients who had undergone ^{18}F-DCFPyL PET/CT studies. These patients were done for primary diagnosis/staging. Positron emission tomography/CT images were analyzed both qualitatively and quantitatively (maximum standardized uptake value (SUVmax) and maximum SUV normalized by lean body mass (SULmax)). Histopathologic diagnosis was taken as reference standard. The optimal cut-off of ^{18}F-DCFPyL was determined using receiver operating characteristic curve (ROC). **Results:** All the patients were confirmed by histopathological examination via prostatectomy or prostate biopsy. Fluorine-18-DCFPyL PET/CT showed higher radiotracer uptake in prostate cancer than that in non-prostate cancer. When SUVmax 5.0 and SULmax 4.0 were cut-off points for determining prostate cancer, the sensitivity of ^{18}F-DCFPyL was 90%, specificity was 100%, and accuracy was 91.2%. Furthermore, there were highly significant positive correlations between SUVmax, SULmax and serum PSA. On comparison of areas under the curve, no significant difference was seen between SUVmax and SULmax in the sensitivity and specificity of ^{18}F-DCFPyL PET/CT for PCa identification. However, delayed PET/CT did not improved accuracy in the term of uncertain PCa in the initial standard imaging. As for lymph node staging, the negative predictive value of ^{18}F-DCFPyL PET/CT was 100%. **Conclusion:** Fluorine-18-DCFPyL PET/CT is a promising imaging modality for initial diagnosis and preoperative N staging in SPCa.

Hell J Nucl Med 2022; 25(1): 11-18 *Epub ahead of print: 8 April 2022* *Published online: 29 April 2022*

Introduction

Prostate cancer (PCa) is one of the most common malignant tumors in men worldwide, with roughly 1,276,106 new cases and 358,989 deaths per year, ranking the third-leading cause of cancer deaths in men [1]. The morbidity and mortality of PCa have showed a clearly upward trend in China [2], probably due to increasingly modern Westernized lifestyle [3].

Prostate cancer was most no symptoms until it is incurable, and useful clinical screening techniques can not currently accurately differentiate between benign and malignant tumors resulting in delaying diagnosis and treatment. Therefore, early diagnosis and accurate staging are key elements for prolonging survival.

Prostate-specific membrane antigen (PSMA), a 750 amino acid transmembrane protein presenting in all prostatic tissues and highly overexpressed (100- to 1,000-fold) on almost all PCa [4], has become increasingly attractive target for imaging and therapy. Radiolabeled small-molecule ligands targeting PSMA can bind to extracellular PSMA active sites to further internalize and recycle in PCa cells but quick clear in non-target tissues, so as to ensure high tumor uptake and high image quality [5, 6]. Currently, several studies have demonstrated that gallium-68 (^{68}Ga)-labelled PSMA tracer (also named ^{68}Ga-PSMA) may be a promising positron emission tomography (PET) probe for imaging PCa including biochemically recurrent prostate cancer (BCR) [7-9]. However, compared with ^{68}Ga, fluorine-18 (^{18}F) may improve imaging of PSMA-expression and is more suitable for clinical application because of a shorter positron range and higher positron yield resulting in higher PET image resolution [10]. Rowe et al. (2016), reported that ^{18}F-labelled PSMA tracers may better improve the detection of small metastases (e.g. at low PSA values) than ^{68}Ga-labelled PSMA traces [11]. Hence, ^{18}F-labeled PSMA tracers have been developed, most notably, ^{18}F-PSMA-1007 ((3S,10S,14S)-1-(4-(((S)-4carboxy-2-

((S)-4-carboxy-2-(6-^{18}F-fluoronicotinamido) butanamido)butanamido)methyl)phenyl)-3-(naphthalen-2-ylmethyl)-1,4,12-trioxo-2,5,11,13-tetraazahexadecane-10,14,16-tricarboxylic acid), and ^{18}F-DCFPyL (2-(3-{1-carboxy-5-[(6-^{18}F-fluoro-pyridine-3-carbonyl)-amino]-pentyl}-ureido)-pent- anedioic acid). Among these ^{18}F-labeled PSMA traces [12, 13], ^{18}F-DCFPyL, a novel PSMA radiotracer, has been indicated to offer early detection of lesions in patients with BCR, even at PSA levels <0.5ng/mL, and revealed enhanced localization of BCR, and is increasingly used in clinical practice of BCR [14, 15]. However, only minimal data are yet available on the diagnostic efficacy in patients with suspected prostate cancer (SPCa) [12]. Hence, the aim of this study was to determine ^{18}F-DCFPyL PET/CT efficacy for lesion detection and N staging in patients with suspected prostate cancer.

Subjects and Methods

Patients

Fifty six SPCa patients who underwent ^{18}F-DCFPyL PET/CT imaging between March 2020 and March 2021 were included in this retrospective study. Exclusion criteria were as followed: Participants with prostate related partial resection or medical treatment; severe patient's condition; unable to lie supine for imaging, unable to provide written consent, exceeding the safe weight of the PET/CT bed (227kg) or unable to fit through the PET/CT bore (70cm diameter). The patient's medical data were collected, including age, Gleason score, TNM-classification, prostate-specific antigen (PSA)-levels, pathology results and clinical follow-up after the ^{18}F-DCFPyL PET/CT scans. The diagnosis of PCa was confirmed by histopathological examination via prostatectomy or prostate biopsy. These patients were performed ^{18}F-DCFPyL PET/CT for diagnosis and staging.

The study protocol was reviewed and approved by the Institutional Review Board of the First Affiliated Hospital of Zhejiang University. Moreover, the study was registered on clinicaltrials.gov (NO. IIT20200015C-R1). All participants provided signed informed consent for participation.

^{18}F-DCFPyL PET/CT imaging

Fluorine-18-DCFPyL was synthesized under good manufacturing practice conditions via direct radiofluoration as previously described [12] at a Siemens Eclipse cyclotron (Siemens Medical Solutions, Knoxville, TN) in the PET center of the First Affiliated Hospital, College of Medicine, Zhejiang University.

Patient doesn't need any specific preparation before injection of ^{18}F-DCFPyL. A dose of 4.44MBq/kg (range 210~450 MBq) was injected intravenously. After the patients rested in a quiet room for 45- to 60-minute, PET/CT imaging was done using a Siemens PET/CT Biograph 16 (Siemens Medical Solutions). Semi-quantitative analysis was done using the maximum standardized uptake value (SUVmax), and maximum standardized uptake value of lean body mass (SULmax), SUVmax and SULmax were calculated using the Syngo volume-counting program (Siemens Medical Solutions). Two experienced nuclear medicine physicians independently reviewed all images.

Statistical analysis

Statistical analysis was performed using SPSS 21.0 software. The nonparametric Wilcoxon signed-rank test was used for comparison of uptake values for 2 related samples. Pearson correlation analysis was used for continuous variables. Receiver- operated characteristic (ROC) curve analysis was used to find the optimal cut-off of SUV parameters. $P<0.05$ was considered significant.

Results

Patients' characteristics

Of these 56 cases (median age, 68y; range, 43-83y), 50 cases (89.3%) were prostate cancer, 4 (7.1%) were normal prostate, 1 (1.8%) was urothelial carcinoma, and 1 (1.8%) was prostatitis. Fluorine-18-DCFPyL PET/CT showed higher radiotracer uptake in prostate cancer than that in non-prostate cancer. These patient characteristics and pathological results are shown in Table 1.

Diagnostic accuracy

Of the 56 cases, 47 patients (83.9%) displayed enhanced ^{18}F-DCFPyL uptake in the prostate or metastasis in visual analysis (median SUVmax 12.8, range 2.8-84.7; median SULmax 8.8, range 2.6-62.1). All the 47 patients with ^{18}F-DCFPyL positive results were confirmed prostate adenocarcinoma by histopathology.

Two patients received secondary biopsies after ^{18}F-DCFPyL PET/CT, within a 2-weeks interval from the primary puncture, to definite diagnosis, since the primary specimens obtained under the guidance of ultrasound did not find cancer cells pathologically. Both 2 cases showed enhanced ^{18}F-DCFPyL uptake in the transitional zone next to the membranous urethra, consistent with the final puncture positive site (Figure 1). It suggested that ^{18}F-DCFPyL PET/CT may help to yield a high diagnostic success rate of biopsy.

Nine patients (16.7%) exhibited uncertain uptake in the prostate by visual analysis, (median SUVmax 3.6, range 2.6-4.8; median SULmax 2.6, range 1.6-4.0). Imaging characteristics of these patients are listed in Table 2. Delayed imaging at 120min were acquired in 5 participants. The value of SUVmax and SULmax in delayed imaging decreased in 1 normal subject, whereas they increased in 1 prostatitis case (Figure 2), 1 PCa patient, 1 with urothelial carcinoma and 1 normal subject. The change of SUVmax (ΔSUVmax, SUVmax at 60min - SUVmax at 120min) and SULmax (ΔSULmax, SULmax at 60min - SULmax at 120min) had no significant difference between PCa and non-PCa.

Semi-quantitative analysis

Receiver operating characteristic (ROC) curves were drawn as Figure 3 only to evaluate the consistency between ^{18}F-DCFPyL PET/CT semi-parameters (SUVmax and SULmax) and pathological findings. When the area under the curve (AUC) of SUVmax and SULmax were 0.922 and 0.925, respectively, the sensitivity and specificity of ^{18}F-DCFPyL PET/CT for PCa identification was no significant difference ($P>0.05$). When the cut-off points of SUVmax and SULmax were 5.0 and 4.0, ^{18}F-DCFPyL PET/CT had

Table 1. *Patient characteristics and pathological results.*

Characteristics	Evaluated Patients, No.	Value (%)
No. of patients	56	
Median age (y)	68 (range 43-83)	
Median tPSA at scanning (ng/mL)	20.4 (range 1.9-1000)	
tPSA(ng/mL)		
<10	16	28.6
10-20	12	21.4
>20	28	50.0
Gleason Score		
6	1	1.8
7	18	32.1
8	18	32.1
9	12	21.4
10	1	1.8
Unknow	6	10.7
Specimen acquisition method		
Operation	25	44.6
Prostate puncture	31	55.4
Pathological Findings		
PCa	50	89.3
Urothelial carcinoma	1	1.8
Normal prostate	4	7.1
Prostatitis	1	1.8

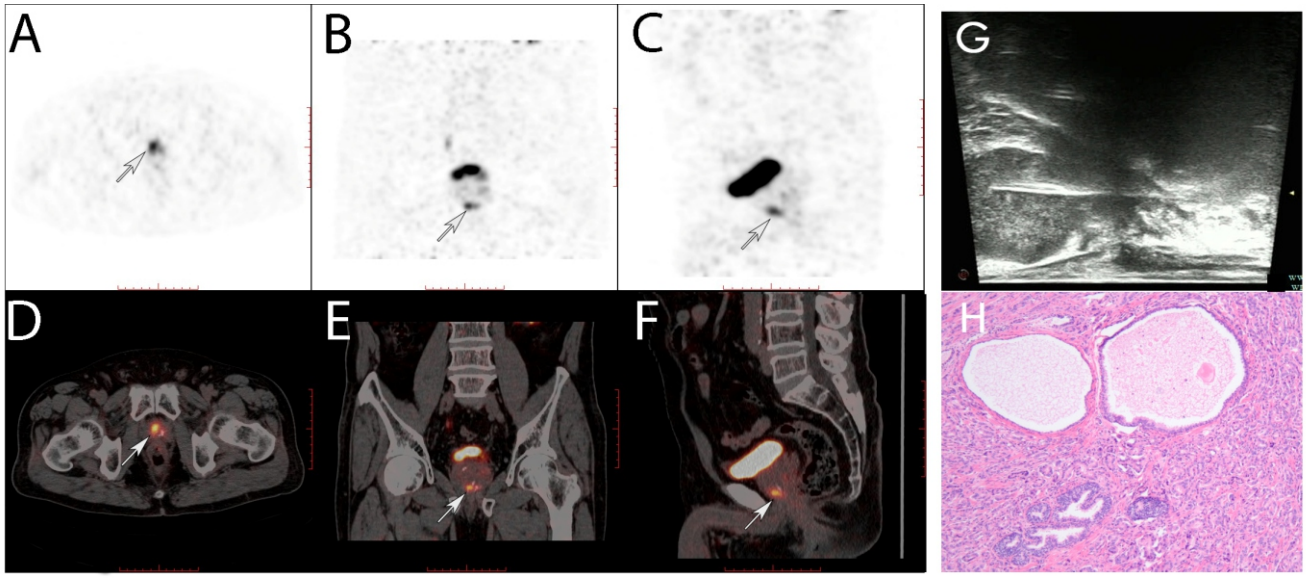

Figure 1. A 74-years-old man patient with suspected prostate cancer (serum PSA 11.8ng/mL) underwent ^{18}F-DCFPyL PET/CT (A-F) for primary diagnosis since the first specimens obtained under the guidance of ultrasound did not find cancer cells pathologically. There was a DCFPyL-avid lesion in the transitional zone next to the membranous urethra (white arrow) in PET images (A-C), axial (A), coronal (B), sagittal (C), and fused PET/CT images (D-F), axial (D), coronal (E), sagittal (F). Secondary ultrasound guided puncture on the DCFPyL-avid lesion (G) showed prostate adenocarcinoma (H).

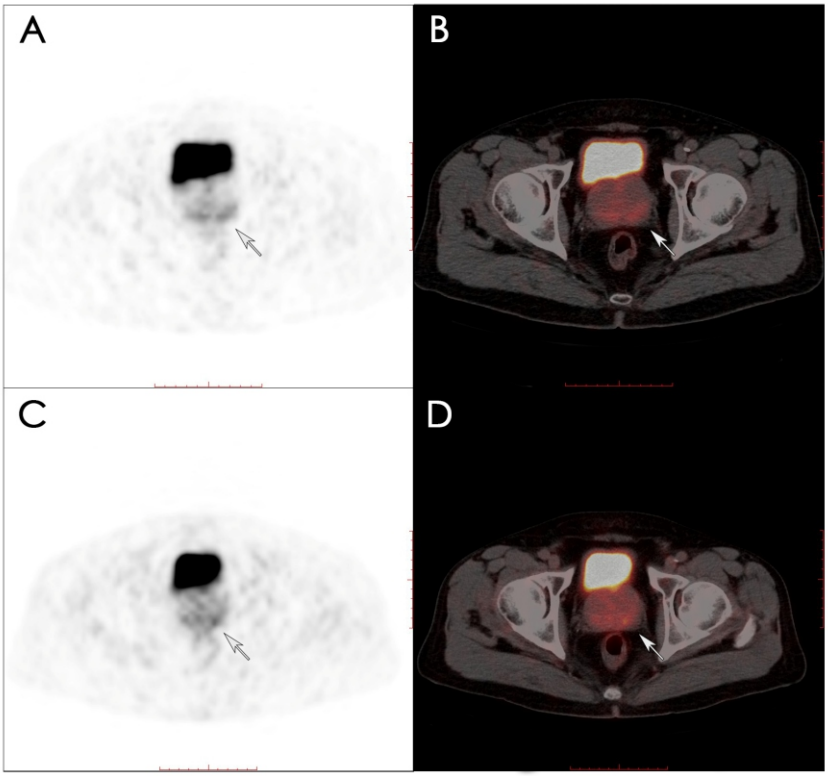

Figure 2. A 67-years-old man patient with suspected prostate cancer (serum PSA 4.5 ng/mL) underwent ^{18}F-DCFPyL PET/CT (A-F) for primary diagnosis. Images of axial PET (A) and PET/CT (B) at 60min after injection showed ambiguous uptake in prostate (white arrow) with SUVmax 4.5 and SULmax 3.4, delayed images of axial PET (C) and PET/CT (D) at 120min showed slightly increased radioactive uptake, with SUVmax 5.3 and SULmax 3.5. The histopathology of biopsies confirmed prostatitis.

Table 2. *Imaging characteristics of these patients.*

Age (y)	Patholoy	tPSA (ng/mL)	SUVmax (60min)	SUVmax (120min)	SULmax (60min)	SULmax (120min)
50	Normal	3.6	3.6	(-)	2.6	(-)
49	Normal	2	4.8	3.7	4.0	2.2
66	Nomal	8.6	4.7	(-)	3.6	(-)
60	Normal	15.5	2.3	2.8	1.6	2.4
67	Prostatitis	4.5	4.2	5.3	3.4	3.5
79	PCa	28.3	2.5	(-)	2.2	(-)
43	PCa	29.1	2.9	(-)	2.2	(-)
56	PCa	1.9	2.8	3.6	2.6	2.5
75	Urothelial carcinoma	2.4	4	4.8	2.6	4.0

true positive in 45 cases (80.4%), true negative in 6 cases (10.7%), false positive in 0 cases (0%), false negative in 5 cases (8.9%). The sensitivity of ^{18}F-DCFPyL was 90%, specificity was 100%, and accuracy was 91.2%.

N (lymph node) staging determination

Of the 56 cases, 25 patients, (24 PCa and 1 urothelial carcinoma), underwent radical prostatectomy and regional lymphadenectomy within one month after ^{18}F-DCFPyL PET/CT. Preoperative ^{18}F-DCFPyL PET/CT showed one metastatic lymph node near the right iliac blood vessel (SUVmax 7.2 and 0.6cm in diameter) in 1 PCa patient (Figure 4) and no metastatic in 23 PCa patients and 1 urothelial carcinoma. Furthermore, out of a total of 106 removed lymph nodes resected, 95 lymph nodes in PCa were confirmed non-metastasis by pathology. The patient with false positive lymph node in ^{18}F-DCFPyL PET/CT was followed up for 4 months, and no lymph node metastasis was found. Fluorine-18-DCFPyL PET/CT had true negative in 23 PCa patients, with a negative predictive value of 100%.

One of the 11 resected lymph nodes was confirmed metastatic lymph node by pathology in urothelial carcinoma, but there was no ^{18}F-DCFPyL uptake.

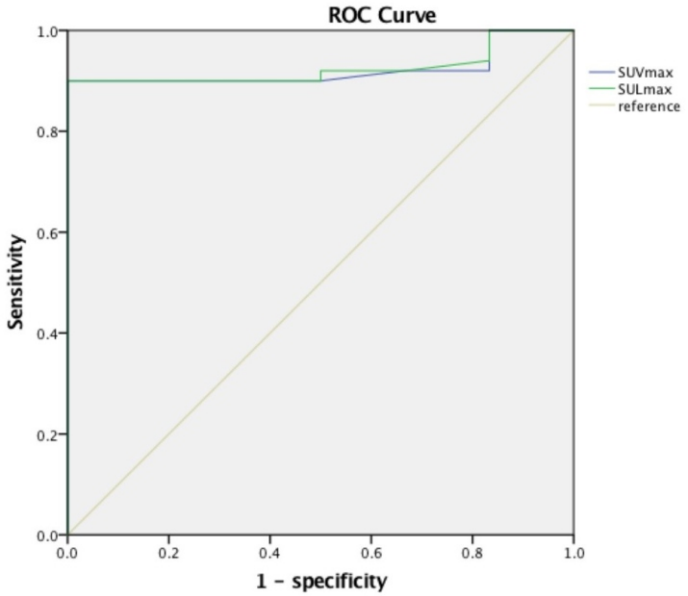

Figure 3. ROC curve of SUVmax and SULmax.

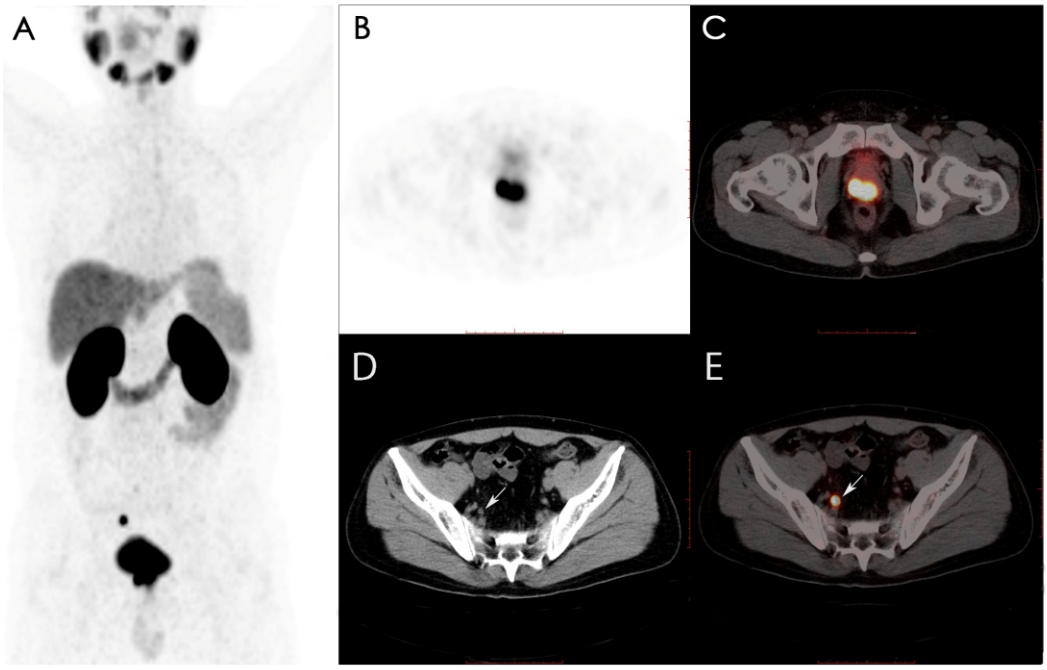

Figure 4. A 49-years-old man patient with suspected prostate cancer (serum PSA 2.0ng/mL) undergoing ^{18}F-DCFPyL PET/CT for primary diagnosis/staging. Positron emission tomography MIP (A) showed increased radioactive in prostate (B, C) and a small lymph node near the right iliac blood vessel (white arrow, D and E) (SUVmax 7.2 and 0.6cm in diameter). Radical prostatectomy specimens demonstrated prostate adenocarcinoma (Gleason 4+5=9) pathologically, and no metastatic lymph node.

Correlation of SUVmax, SULmax and serum PSA

Maximum SUV and SULmax in the patients with increased serum PSA (>10ng/mL) were significantly higher than those in low serum PSA level (<10ng/mL) (6.95±3.95 vs. 20.3±15.9, P=0.009) and (5.32±3.01 vs. 14.52±14.19, P=0.013), respectively.

According to the level of serum PSA, 56 patients were divided into normal PSA group (5 cases), PSA 4-10ng/mL group (11 cases), PSA 10-20ng/mL group (12 cases), and PSA >20ng/mL group (28 cases). Maximum SUV in normal PSA group, 4-10ng/mL group ,10-20ng/mL group, and >20ng/mL group were 4.0 (range 2.8-15.6), 6.3 (range 2.3-13.6), 12.3 (range 2.3-53.4), 14.0 (range 2.9-84.7), and SULmax in the four group were 2.8 (range 2.2-12.3), 5.0 (range 2.2-9.8), 7.6 (range 1.6-30.9), and 10.5 (2.2-62.1), respectively. The correlations between SUVmax, SULmax and serum PSA level were displayed in Figure 5 and Figure 6.

The diagnostic accuracy of ^{18}F-DCFPyL PET/CT in SPCa with increased PSA level (>10ng/mL) was 97.5% and 87.5% with low serum PSA level (<10ng/mL).

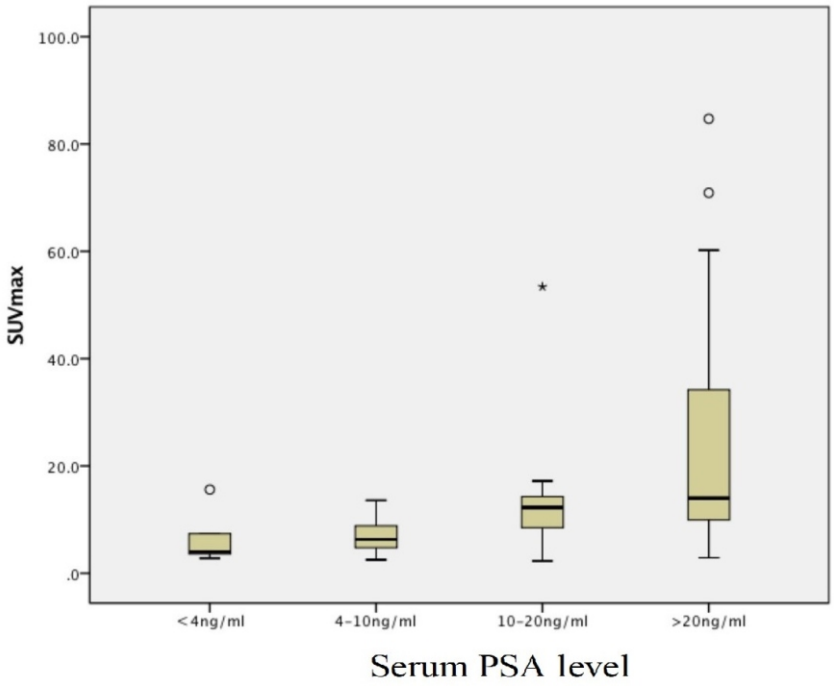

Figure 5. The correlations between SUVmax and serum PSA level.

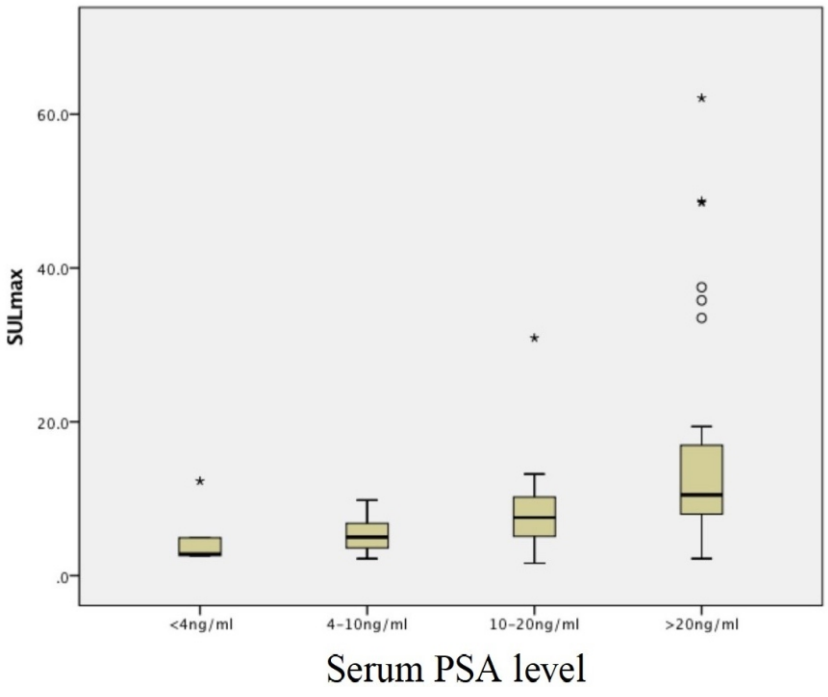

Figure 6. The correlations between SULmax and serum PSA level.

Discussion

The prostate-specific antigen (PSA), which is almost expressed in prostate, is secreted into the seminal fluid rather than into the circulation under normal physiological conditions [16]. Increase serum PSA levels are commonly guided by benign prostate hyperplasia (BPH) or neoplasia, owing to the disruption of the prostate gland's architecture, followed by the leakage of PSA into the circulatory system. According to the commonly used cut-off value of 4.1ng/mL, it has reported a 6.2% false-positive rate and low sensitivity (20.5%) for detecting cancer cases [17]. Jemaa et al. (2013), found that PSMA was weakly expressed in BPH, which made PSMA more target potential than PSA in primary prostate carcinomas [18]. Fluorine-18-DCFPyL, as a promising radiotracer targeting PSMA, has been reported to offer early detection and high detection rates in BCR, which could localize 47.6%-60% positive recurrent prostate cancer even with PSA levels less than 0.5ng/mL [10, 14, 15]. Meanwhile, Wondergem et al. (2021) reported that ^{18}F-DCFPyL PET/CT detected 48% additional metastatic lymph nodes without enlarged sizes on CT and altered therapeutic management in 17% of patients [19]. In this present study, ^{18}F-DCFPyL PET/CT demonstrates favorable diagnostic accuracy in SPCa diagnosis and 100% negative predictive value in LN staging. As to urothelial carcinoma, neither the primary focus nor the metastatic lymph node showed enhanced radioactive uptake, probably due to negligible tumor neovascularization and weak expression of PSMA [20].

Areas of the curves (AUC) of SUVmax and SULmax were 0.922 and 0.925 respectively, showing no significant difference for PCa identification. When SUVmax 5.0 and SULmax 4.0 were cut-off points for determining prostate cancer, the sensitivity, specificity and accuracy of ^{18}F-DCFPyL were 90%, 100% and 91.2%, respectively. One hundred twenty min delayed-time point images, which are mostly being used for distinction between inflammatory and malignant diseases in ^{18}F-fluorodeoxyglucose (FDG) PET/CT [21], do not improve accuracy in the term of uncertain PCa in the initial standard imaging in this study. Necessary biopsies are still recommended for patients with negative results.

In this study, 3 patients with PCa (6%) did not demonstrate enhanced ^{18}F-DCFPyL radioactive uptake, consistent with the 5%-10% negative result in previous study [22]. There were highly significant positive correlations between SUVmax, SULmax and serum PSA. Almost identified with the earlier study of ^{68}Ga labelled radiotracer (^{68}Ga-PSMA-11) PET/CT, patients also exhibited statistically higher uptake in PSA ≥10.0ng/mL than PSA <10.0ng/mL in ^{68}Ga-PSMA-11 PET/CT [23]. The detection rate of ^{18}F-DCFPyL in BCR also increased with the rise of PSA levels [11]. These findings are further supported by previous literature demonstrating elevated immunohistochemical expression and enzymatic activity of PSMA in advanced PCa [24].

Two (4%) cases received secondary biopsies under the guidance of ^{18}F-DCFPyL PET/CT due to the unrepresentative specimens by primary ultrasound guided puncture. The concerns on sample representativeness are always challenges faced with pathology and a series of studies try to elevate the accuracy of biopsies [25, 26]. Fluorine-18-DCFPyL PET/CT not only exhibited similar sensitivity and tumor detection rate to multi-parameter MRI (mpMRI) in patients with high-risk PCa, (PET/CT, 90.9% and 80%; mpMRI, 86.4% and 88.4%; P=0.58/0.17), but also could detect tumors missed on mpMRI [27]. Gallium-68-PSMA-guided bone biopsies are reported to provide more success rate than CT-guided biopsy in metastatic PCa (70% vs. 40%) [28]. Importantly, the time (2-week intervals) between biopsy and ^{18}F-DCFPyL imaging do not have any influence on the accuracy of image interpretation, suggesting that ^{18}F-DCFPyL imaging is superior to mpMRI in the determination of imaging time after biopsy [29].

Major limitations of the present study are the retrospective design and the small number of patients enrolled from a single institution. A prospective multicenter trial with a larger cohort would make a strong argument on the exact role of ^{18}F-DCFPyL PET/CT for initial diagnosis and preoperative staging in SPCa.

In conclusion, ^{18}F-DCFPyL PET/CT is a promising imaging modality for initial diagnosis and preoperative staging in the patients with prostate cancer. Necessary biopsies are still recommended for SPCa patients with negative results.

Funding

The author(s) disclosed receipt of the following financial support for the research, authorship, and/or publication of this article: Sponsored by National Natural Science Foundation of China (NSFC) (82071965), Fujian medical innovation project (2019-CXB-32) and National Natural Science Foundation of Fujian province (2020J011210).

The authors declare that they have no conflicts of interest.

Bibliography

1. Freddie, Bray, Jacques et al. Global cancer statistics 2018: GLOBOCAN estimates of incidence and mortality worldwide for 36 cancers in 185 countries. *CA Cancer J Clin* 2018; 68 (suppl 8): 394-424.
2. Chen W, Zheng R, Baade P D et al. Cancer statistics in China, 2015. *CA Cancer J Clin* 2016; 66(2): 115-32.
3. Baade P D, Youlden D R, Krnjacki L J. International epidemiology of prostate cancer: geographical distribution and secular trends. *Mol Nutr Food Res* 2009; 53(2): 171-84.
4. Bostwick D G, Pacelli A, Blute M et al. Prostate specific membrane antigen expression in prostatic intraepithelial neoplasia and adenocarcinoma: a study of 184 cases. *Cancer* 1998; 82(11): 2256-61.
5. Schwarzenb Ck S M, Rauscher I, Bluemel C et al. PSMA ligands for PET imaging of prostate cancer. *J Nucl Med* 2017; 58 (10): 1545-52.
6. Chen Y, Foss C A, Byun Y et al. Radiohalogenated prostate-specific membrane antigen (PSMA)-based ureas as imaging agents for prostate cancer. *J Med Chem* 2008; 51(24): 7933-43.
7. Maurer T, Eiber M, Schwaiger M et al. Current use of PSMA-PET in prostate cancer management. *Nat Rev Urol* 2016; 13(4): 226-35.
8. Fendler W P, Calais J, Eiber M et al. Assessment of ^{68}Ga-PSMA-11 PET Accuracy in Localizing Recurrent Prostate Cancer: A Prospective Single-Arm Clinical Trial. *JAMA Oncol* 2019; 5(6): 856-63.
9. Calais J, Ceci F, Eiber M et al. ^{18}F-fluciclovine PET-CT and ^{68}Ga-PSMA-11 PET-CT in patients with early biochemical recurrence after prostatectomy: a prospective, single-centre, single-arm, comparative imaging trial. *The Lancet Oncol* 2019; 20(9): 1286-94.
10. Wondergem M, Jansen B, Zant F et al. Early lesion detection with ^{18}F-DCFPyL PET/CT in 248 patients with biochemically recurrent prostate cancer. *Eur J Nucl Med Mol Imaging* 2019; 46(9): 1911-8.

11. Rowe S P, Gorin M A, Allaf M E et al. PET imaging of prostate-specific membrane antigen in prostate cancer: current state of the art and future challenges. *Prostate Cancer Prostatic Dis* 2016; 19(3): 223-30.
12. Szabo Z, Mena E, Rowe S P et al. Initial Evaluation of ^{18}F-DCFPyL for Prostate-Specific Membrane Antigen (PSMA)-Targeted PET Imaging of Prostate Cancer. *Mol imaging Biol* 2015; 17(4): 565-74.
13. Giesel F L, Hadaschik B, Cardinale J et al. F-18 labelled PSMA-1007: biodistribution, radiation dosimetry and histopathological validation of tumor lesions in prostate cancer patients. *Eur J Nucl Med Mol Imaging* 2017; 44(4): 678-88.
14. Rousseau E, Wilson D, Lacroix-Poisson F et al. A prospective study on ^{18}F-DCFPYL PSMA PET/CT imaging in biochemical recurrence of prostate cancer. *J Nucl Med* 2019; 60(11): 1587-93.
15. Mena, Esther, Lindenberg et al. ^{18}F-DCFPyL PET/CT Imaging in Patients with Biochemically Recurrent Prostate Cancer After Primary Local Therapy. *J Nucl Med* 2020; 61(6): 881-89.
16. Moradi A, Srinivasan S, Clements J et al. Beyond the biomarker role: prostate-specific antigen (PSA) in the prostate cancer microenvironment. *Cancer Metastasis Rev* 2019; 38(3): 333-46.
17. Thompson I M, Ankerst D P, Chi C et al. Operating Characteristics of Prostate-Specific Antigen in Men Withan Initial PSA Level of 3.0ng/mL or Lower. *Jama* 2005; 294(1): 66-70.
18. Jemaa A B, Bouraoui Y, Sallami S et al. Cellular distribution and heterogeneity of Psa and Psma expression in normal, hyperplasia and human prostate cancer. *Tunis Med* 2013; 91(7): 458-63.
19. Wondergem M, Zant F, Broos W et al. ^{18}F-DCFPyL PET/CT for primary staging in 160 high-risk prostate cancer patients; metastasis detection rate, influence on clinical management and preliminary results of treatment efficacy. *Eur J Nucl Med Mol Imaging* 2021; 48(2): 521-31.
20. Campbell S P, Baras A S, Ball M W et al. Low levels of PSMA expression limit the utility of ^{18}F-DCFPyL PET/CT for imaging urothelial carcinoma. *Ann Nucl Med* 2018; 32(1): 69-74.
21. Houshmand S, Salavati A, Segtnan E A et al. Dual-time-point Imaging and Delayed-time-point Fluorodeoxyglucose-PET/Computed Tomography Imaging in Various Clinical Settings. *PET Clin* 2016; 11(1): 65-84.
22. Budaus L, Leyh-Bannurah S R, Salomon G. Initial experience of ^{68}Ga-PSMA PET/CT imaging in high-risk prostate cancer patients prior to radical prostatectomy. *Eur Urol* 2016; 69(3): 393-6.
23. Uprimny C, Kroiss A S, Decristoforo C et al. ^{68}Ga-PSMA-11 PET/CT in primary staging of prostate cancer: PSA and Gleason score predict the intensity of tracer accumulation in the primary tumour. *Eur J Nucl Med Mol Imaging* 2017; 44(6): 941-9.
24. Lapidus R G, Tiffany C W, Isaacs J T et al. Prostate-specific membrane antigen (PSMA) enzyme activity is elevated in prostate cancer cells. *Prostate* 2000; 45(4): 350-4.
25. Drost FJH, Osses DF, Nieboer D et al. Prostate MRI, with or without MRI-targeted biopsy, and systematic biopsy for detecting prostate cancer. *Cochrane Database Syst Rev* 2019; 4(4): CD012663.
26. Cheung D C, Li J, Finelli A. A narrative review and update on management following negative prostate biopsy. *Curr Opin Urol* 2018; 28(4): 398-402.
27. Gaur S, Mena E, Harmon S A et al. Prospective evaluation of ^{18}F-DCFPyL PET/CT in detection of high-risk localized prostate cancer: Comparison with mpMRI. *Am J Roentgenol* 2020; 215(3): 652-9.
28. Jong A C D, Smits M, Riet J V et al. ^{68}Ga-PSMA guided bone biopsies for molecular diagnostics in metastatic prostate cancer patients. *J Nucl Med* 2020; 61(11): 1607-14.
29. White S, Hricak H, Forstner R et al. Prostate cancer: effect of postbiopsy hemorrhage on interpretation of MR images. *Radiol* 1995; 195(2): 385-90.